ELM Characterization and Dynamics at Near-Unity A in the Pegasus ST

M.W. Bongard[1], J.L. Barr[1], R.J. Fonck[1], D.M. Kriete[1], J.A. Reusch[1], K.E. Thome[1,2]

[1]University of Wisconsin-Madison, Madison, WI, USA

[2]Oak Ridge Associated Universities, Oak Ridge, TN, USA

E-mail contact of main author: mbongard@wisc.edu

Abstract. Operation in the high confinement (H-mode) regime and mitigation of associated deleterious Edge Localized Mode (ELM) activity are necessary for the success of ITER and future reactors. H-mode studies at near-unity aspect ratio A can offer unique insights into these issues. Edge plasma parameters at low A permit unique measurements of the edge pedestal with high spatiotemporal resolution using probes. In particular, measurements of the current density profile J_{edge} of import to peeling-ballooning stability and its nonlinear dynamics during ELMs are presented. Two classes of ELMs have been identified to date by their proximity to P_{LH} and measured n spectra provided by a near-edge Mirnov coil array. Both ELM types produce propagating, field-aligned filaments and have multiple n measured during the crash. These observations are consistent with the presence of a spectrum of simultaneously unstable peeling-ballooning modes anticipated by theory and nonlinear ELM simulations. Small, Type III-like ELMs occur at $P_{IN} \sim P_{LH}$ with $n \leq 4$. Large, Type I-like ELMs occur with $P_{IN} > P_{LH}$ and intermediate $5 < n < 15$, similar to ELMs at $A \sim 1.3$ in NSTX. The Type III n ranges are opposite that reported at high A, and Type I n are in the low range of those reported at high A. These differences presumably reflect the strong peeling mode drive $\sim J_{edge}/B$ present in the ST. The dominant n component of a large ELM grows exponentially, whereas other n are nonlinearly driven and damped prior to the crash. Access to small and large ELMs are demonstrated in Ohmic H-mode plasmas by varying the applied input power. $J_{edge}(R,t)$ measurements have been obtained across single ELM events with sub-cm spatial and Alfvénic temporal resolution. Both ELM types feature the nonlinear generation of "current-hole" J_{edge} perturbations, similar to prior studies of nonlinear peeling mode dynamics in Pegasus. A Type I ELM is shown to additionally expel a current-carrying filament during the ELM crash. Experiments coupling small amounts of helical edge current injection to H-mode plasmas find suppression of Type III ELM activity and negligible macroscopic impact on the discharge. This occurs for injected currents $I_{inj} \leq 1$ kA. Above $I_{inj} \geq 1$ kA the 3D field perturbation degrades the edge sufficiently to exit H-mode.

1. Introduction

Operation in the high confinement (H-mode) regime and effective mitigation of associated deleterious Edge Localized Mode (ELM) activity is necessary for the success of ITER and future tokamak-based reactors. ELMs eject plasma particles and energy to vessel structures on Alfvénic timescales ($\leq$ 100 μs). The transient heat loads and potential impurity influxes associated with ELMs in burning plasma devices can readily lead to material damage, loss of thermal management in a detached divertor, fuel dilution, radiative losses, or even plasma disruption. These concerns have focused worldwide efforts to understand the underlying physical mechanisms associated with ELM events and develop effective strategies to suppress or mitigate these effects. Detailed edge measurements with fine spatial and Alfvénic temporal resolution are critical to the experimental validation of nonlinear ELM physics models and simulations [1].

H-mode studies in the ultra-low aspect ratio regime ($A < 1.3$) test the understanding of ELMs in configurations with extreme toroidicity and allow unique measurements of the edge current and pressure profiles that determine ELM peeling-ballooning stability [2]. This paper

describes experimental results characterizing ELMs in Ohmic H-mode plasmas in the Pegasus Toroidal Experiment [3], their relation to higher aspect ratio configurations, and unique measurements of ELM activity, including current profile dynamics, facilitated by the $A \sim 1$ ST configuration.

Section 2 describes the means used to access to ELMy H-mode plasmas in Pegasus, the diagnostic measurements and analysis used to characterize them, and features of the observed ELMs with respect to common classification metrics. Section 3 reports on nonlinear ELM dynamics, including magnetic precursor behavior and unique, time-resolved measurements of the edge current profile during single ELM events. Section 4 presents the results of an experiment that modified small ELM onset by introduction of strong helical current drive in the edge. Section 5 summarizes the observations and describes opportunities for future work.

2. ELM Characterization

2.1. Access and Diagnosis

Pegasus is an extremely low aspect ratio spherical tokamak, with major parameters R = 0.25–0.45 m, A = 1.15–1.3, elongation = 1–3, $I_p \sim 0.25$ MA, $B_T < 0.2$ T, $I_N \leq 14$, and $l_i \leq 0.6$. This very low B_T reduces the L-H power threshold, P_{LH}, such that H-mode plasmas are attainable with Ohmic heating alone in limited and diverted magnetic topologies [2]. In addition, high-field-side neutral fueling is commonly utilized to facilitate the L-H transition. H-modes have also been achieved following non-solenoidal local helicity injection (LHI) startup [4,5]. Plasmas described here were operated with deuterium as the main ion species.

ELMs are regularly observed in Pegasus H-mode plasmas. They transiently destroy the H-mode edge and generate characteristic bursts of D_α emissions (sampled with 1 MHz temporal resolution) that are temporally correlated with the creation of propagating, field-aligned filaments on fast visible imaging with a Phantom v12 camera. Two classes of ELMs have been identified to date, and detailed further below. Figure 1 shows representative visible images attained with exposure times $\Delta t_{exp} \sim 10$ μs of: a diverted H-mode plasma [Fig. 1(a)], with the bright spots on the center column being the location of high-field-side fueling; a contrast-enhanced image of a dim, small ELM in a limited discharge [Fig. 1(b)]; and a bright, large ELM [Fig. 1(c)] that features a spiral heat deposition pattern on the upper and lower divertor plates. Irregularly-spaced filaments are commonly observed, suggesting nonlinear interaction of edge peeling-ballooning modes may be occurring [1,6,7].

In addition to standard external spectroscopic, magnetic, and fast imaging diagnostics, the short pulse lengths (~20 ms) and modest edge T_e in the device permit detailed, direct

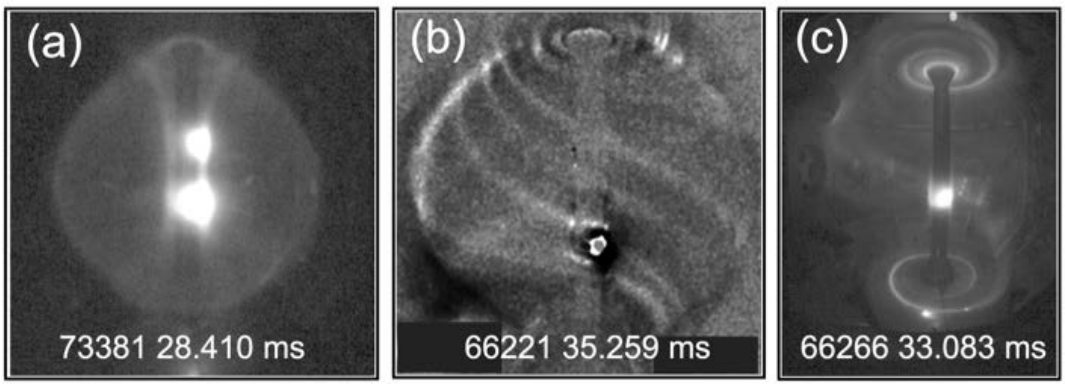

FIG. 1. Fast visible images of (a) diverted H-mode, (b) small ELM (contrast enhanced) and (c) large ELM.

measurements in the edge pedestal region using internal probes with high spatial and temporal resolution.

Edge current profiles $J_{edge}(R, t)$ are provided by a radially scanning, sixteen-channel array of Hall effect sensors oriented to measure $B_Z(R,t)$ in the plasma edge with 7.5 mm spatial resolution [8]. A refined temporal calibration of the diagnostic has indicated sensitivity to magnetic fluctuations up to 175 kHz (Δt ~ 6 μs). In these experiments, the Hall probe was positioned at Z = 0 cm to sample the edge poloidal field directly (*i.e.*, $B_p = B_Z$). Such measurements may be related to the local toroidal current density $J_\phi(R,t)$ with comparable time resolution via Ampère's Law. The local B_R term is eliminated by virtue of the sensor measurement locations, and its Z derivative is estimated from the available $B_Z(R)$ data under the assumption of local Grad-Shafranov equilibrium [9–11].

ELM MHD activity is measured with 1 MHz bandwidth using an insertable toroidal Mirnov coil array. It can be positioned up to ~1 cm outside the plasma boundary at the device midplane (Z = 0 cm). Six coils that measure B_Z are placed in a linear array and oriented tangent to the plasma boundary, spanning approximately 15° in toroidal angle when $R_{probe} \sim R_{edge}$. Standard Fourier analysis techniques allow the computation of two-point spectral estimators (cross-power $\hat{P}$, cross-phase $\hat{\theta}$, and coherence $\hat{\gamma}^2$) between coil pairs to identify coherent electromagnetic activity. Instability toroidal mode numbers, n, are readily inferred from a multipoint linear fit of measured cross-phase as a function of sensor toroidal angle.

2.2. ELM Classification

Two types of ELMs have been observed in Pegasus to date. Application of conventional ELM classification metrics utilizing the ELM frequency-power relationship [12] is not possible in these Ohmic discharges due to the lack of available auxiliary heating. They are nonetheless clearly distinguished by their occurrence at different values of $P_{IN} = P_{OH} - dW/dt - P_{RAD}$ with respect to P_{LH} and their measured magnetic n spectra. Here, $P_{OH} = I_p V_{loop}$ is the applied Ohmic input power, W is the sum of the equilibrium kinetic and magnetic stored energy, and P_{RAD} denotes radiative losses. Small, Type III-like ELMs are present at $P_{IN} \sim P_{LH}$. As P_{IN} is increased, large, Type-I-like ELMs with intermediate n occur. Large ELM virulence increases with additional P_{IN}, potentially terminating discharges when $P_{IN}/P_{LH} \gtrsim 2$.

Figure 2 demonstrates a discharge that transitions from the small, Type III ELM regime to the large, Type I ELM regime by varying the applied Ohmic input power. The plasma current is shown in Fig. 2(a), which features a strong ramp from ~24–28 ms under conditions of constant loop voltage. Estimates for the applied input power and L-H transition power are provided in Fig. 2(b). Equilibrium reconstructions indicate that $P_{IN}(t)$ (solid red line) can reasonably be estimated for many Pegasus H-mode plasmas by approximating dW/dt as (0.4 ± 0.1) P_{OH} (shaded bands) and neglecting radiative losses [5]. $P_{LH}(t)$ (dashed black) is estimated based

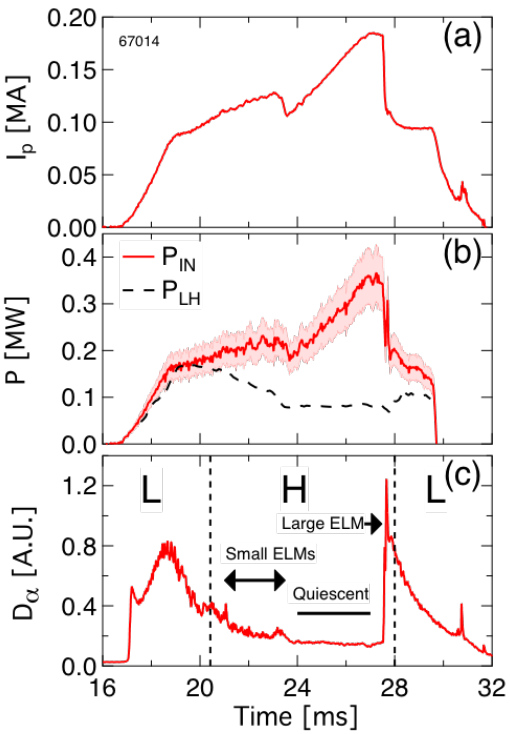

FIG. 2. I_p (a), P_{IN} and estimated P_{LH} (b), and D_α waveforms (c) in discharge with small and large ELMs.

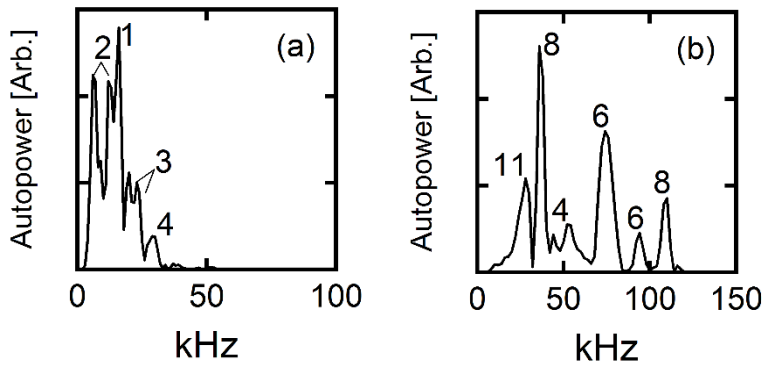

FIG. 3. Autopower spectra and n of small, Type III (a) and large, Type I (b) ELMs [2].

on recent results [2] that suggest the L-H transition power at $A \sim 1.2$ in Pegasus is consistent with a 15× enhancement over that predicted by the empirical 2008 ITPA P_{LH} scaling expression developed for ITER [13]. Figure 2(c) shows a D_α filterscope signal and indicators of the discharge phase and temporal regions corresponding to observed ELM activity.

As the input power is increased above $P_{LH} \sim 0.2$ MW near 20 ms, an H-mode transition occurs. Immediately thereafter, frequent Type III ELMs are observed. They are reflected in the D_α signal by small spikes that coincide with filament bursts on visible imaging which are similar to those depicted in Fig. 1(b). As P_{IN} is increased further, ELM activity ceases, leading to a ~4 ms quiescent period that is also free of low-*n* core tearing mode activity. This period is terminated by the onset of a virulent Type I ELM at 27.5 ms when $P_{IN}/P_{LH} \sim 3$. This particular high-power ELM appears to stimulate an H-L back-transition due to the large drop in I_p at the event. At lower P_{IN}, I_p is less affected and similar Type I ELMs do not cause back-transitions.

Both ELM types generate observable magnetic precursors. Multiple *n* are observed during ELMs, consistent with the presence of simultaneously unstable peeling-ballooning modes expected by theory [14] and observed in nonlinear simulations [1,6]. Magnetic autopower spectra and *n* identified from multipoint cross-phase spectral analysis [9] of single ELM events are shown in Fig. 3. Type III ELMs are shown to have $n \leq 4$ [Fig. 3(a)], whereas Type I ELMs have intermediate $5 < n < 15$ present [Fig. 3(b)]. Such mode numbers are similar to those observed in Type III and Type I ELMs, respectively, at $A \sim 1.3$ in NSTX [15]. However, the mode numbers for both ELM classes in Pegasus are systematically lower than those observed at high *A* [16]. This difference is presumably due to the higher intrinsic peeling instability drive ($\propto J_{edge}/B$) arising at low aspect ratio [10,11].

3. Nonlinear ELM Dynamics

Predicting the consequences of exciting an ELM via peeling-ballooning instability such as the magnitude, frequency, and spatial localization of particle and energy fluxes fundamentally requires a nonlinear treatment [1]. Unlike core instabilities that are localized to a particular unstable resonant surface, peeling-ballooning modes are generally simultaneously unstable to a spectrum of *n*, each of which has differing growth rates that themselves may be dependent on the instantaneous value of the (collapsing) pedestal pressure, current, and flow profiles. The temporal evolution of these time-varying toroidal harmonics has been attributed in nonlinear theory and simulation [1,14] to generate the propagating 3D filaments observed in experiment during an ELM crash. High spatiotemporal resolution measurements of edge profiles and edge-localized magnetic fluctuation measurements are identified as critical to validating nonlinear ELM simulations [1]. Measurements of edge current profile dynamics, in particular, represent a gap in our efforts to predictively understand the full ELM cycle.

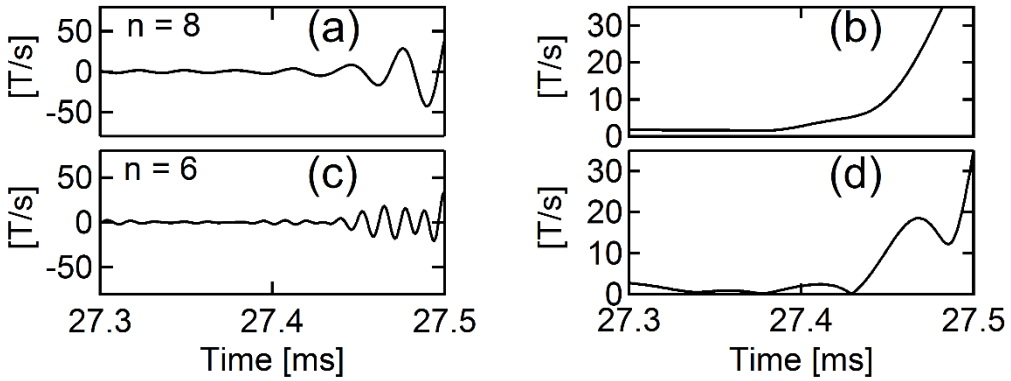

FIG. 4. Type I ELM magnetic precursors: 35 kHz n = 8 dB_Z/dt (a) and envelope function (b); 75 kHz n = 6 dB_Z/dt (c) and envelope function (d).

Nonlinear ELM magnetic precursors are clearly observed on the near-edge Mirnov array. Figs. 4(a)–(d) show bandpass-filtered Mirnov dB_Z/dt signals [(a), (c)] and their amplitudes [(b), (d)] calculated via the Hilbert transform that document the time evolution of the dominant 35 kHz n = 8 mode and a representative sub-dominant 75 kHz n = 6 mode in a 500 μs period preceding the measured D_α rise of a large ELM. The n = 8 mode grows continuously through the time period. In contrast, the n = 6 mode evolves nonlinearly, growing and damping prior to the ELM crash.

The high spatiotemporal resolution of the Pegasus Hall probe and simplified diagnostic pedestal access at low A allows unique measurements of nonlinear ELM dynamics [2]. Edge current profile measurements (Fig. 5) have been obtained across single ELMs with sub-cm spatial and Alfvénic temporal resolution, documenting their complex nonlinear evolution. Figure 5(a) shows $J_{edge}(R,t)$ before (solid red), during (dashed purple), and after (solid grey) a Type III ELM. A "current-hole" J_{edge} perturbation is coincident with D_α spikes and strong magnetic fluctuation activity, similar to the nonlinear evolution of peeling modes on Pegasus [10]. $J_{edge}(R,t)$ from a single Type I ELM is shown in Fig. 5(b). The peak J_{edge} (solid red) transiently relaxes to an L-mode-like, wider pedestal gradient (dashed purple), followed by the formation and ejection of a current filament (hashed green) that accelerates from the post-ELM edge (solid black). The inferred filament generation is temporally coincident with an outwardly-propagating filament at the Hall sensor location as determined from visible imaging. The generation and expulsion of such filaments due to peeling-ballooning instabilities are postulated by electromagnetic blob transport theory and are observed in nonlinear simulations of ELMs [2,5].

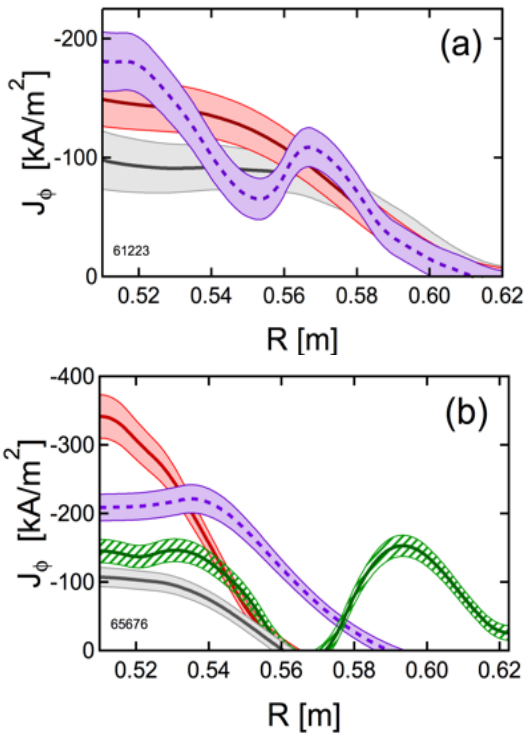

FIG. 5. $J_{edge}(R,t)$ evolution during single ELM events. Type III ELM with current-hole (a); (b) Type I ELM with filament expulsion.

4. ELM Modification via Helical Current Drive

Leveraging the edge current injectors normally used for nonsolenoidal startup, but at lower power, may afford a novel means of ELM modification through helical edge magnetic perturbations [5]. Figure 6 shows initial investigations of the effects of injecting perturbing helical current streams with varied injector current I_{inj} several cm outside the edge pedestal region along open field lines in the scrapeoff layer adjoining an H-mode plasma. This is conceptually similar to experiments conducted on EAST [17], where the helical edge current injection was established via RF current drive instead of helicity injectors.

At relatively low $I_{inj} \leq 1$ kA, no effects on the plasma current [Fig. 6(a)] or diamagnetic flux loop measurement Φ_D [Fig. 6(b)] are evident. However, a marked decrease in the Type III ELM activity occurs, as illustrated by reduced high-frequency D_α bursts in Figs. 6(c)–(d). For $I_{inj} > 2$ kA, a strong drop in I_p and Φ_D is evident as increasing perturbing field is applied, consistent with very strong perturbations of the edge and loss of H-mode confinement.

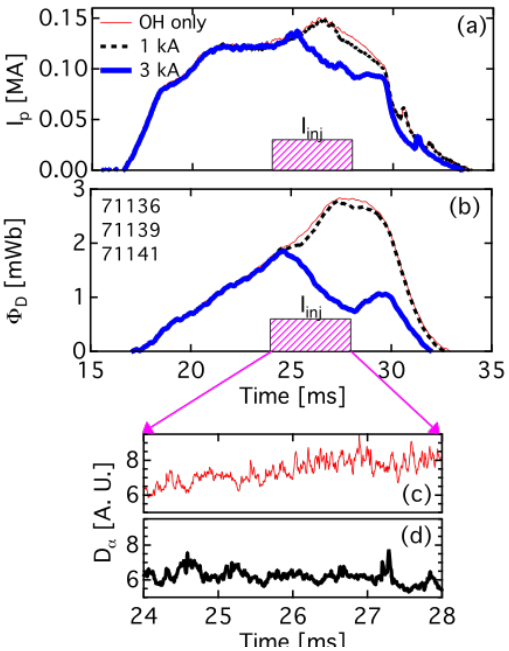

FIG. 6. H-mode plasmas perturbed with helical edge current injection. I_p (a), Φ_D (b), and $D_\alpha(t)$ for cases with I_{inj} = 0 kA (c), I_{inj} = 1 kA (d).

5. Summary and Discussion

Edge localized modes are readily accessed in Ohmic H-mode plasmas at near-unity aspect ratio in the Pegasus Toroidal Experiment. Their input power dependencies, measured magnetic toroidal mode number spectra, and field-aligned filament generation are consistent with observations in other high-performance devices. In conjunction with the modest edge parameters present at $A \sim 1$, highly resolved, unique measurements of nonlinear ELM dynamics are enabled on the Alfvénic timescales of the instability of import to validation of ELM models [1]. Initial experiments exploring 3D magnetic field perturbations with helical edge current stream injection were found to reduce Type III ELM activity.

These and future measurements can provide rich opportunities to test nonlinear simulations of ELMs in high-performance fusion plasmas.

This material is based upon work supported by the U.S. Department of Energy, Office of Science, Office of Fusion Energy Sciences, under Award Number DE-FG02-96ER54375. Disclaimer: Any opinions, findings, and conclusions or recommendations expressed in this publication are those of the authors and do not necessarily reflect the views of the U.S. Department of Energy.

[1] HUIJSMANS, G.T.A., et al., “Modelling of edge localised modes and edge localised mode control,” Phys. Plasmas **22** (2015) 021805.

[2] THOME, K.E., et al., “High Confinement Mode and Edge Localized Mode Characteristics in a Near-Unity Aspect Ratio Tokamak,” Phys. Rev. Lett. **116** (2016) 175001.

[3] GARSTKA, G.D., et al., “The upgraded Pegasus Toroidal Experiment,” Nucl. Fusion **46** (2006) S603.

[4] BATTAGLIA, D.J., et al., “Tokamak startup using outboard current injection on the Pegasus Toroidal Experiment,” Nucl. Fusion **51** (2011) 073029.

[5] THOME, K.E., et al., H-mode plasmas at very low aspect ratio on the Pegasus Toroidal Experiment, Nucl. Fusion (in press).

[6] SUGIYAMA, L.E., “Mode coupling and aspect ratio effects on low and high-*n* plasma instabilities,” Nucl. Fusion **55** (2015) 073006.

[7] PAMELA, S.J.P., et al., “Resistive MHD simulation of edge-localized-modes for double-null discharges on the MAST device,” Plasma Phys. Control. Fusion **55** (2013) 095001.

[8] BONGARD, M.W., et al., “A Hall sensor array for internal current profile constraint,” Rev. Sci. Instrum. **81** (2010) 10E105.

[9] PETTY, C.C., et al., “Analysis of current drive using MSE polarimetry without equilibrium reconstruction,” Nucl. Fusion **42** (2002) 1124.

[10] BONGARD, M.W., et al., “Measurement of Peeling Mode Edge Current Profile Dynamics,” Phys. Rev. Lett. **107** (2011) 035003.

[11] BONGARD, M.W., et al., “Characterization of peeling modes in a low aspect ratio tokamak,” Nucl. Fusion **54** (2014) 114008.

[12] ZOHM, H., “Edge localized modes (ELMs),” Plasma Phys. Control. Fusion **38** (1996) 105.

[13] MARTIN, Y.R., et al., “Power requirement for accessing the H-mode in ITER,” J. Phys.: Conf. Ser. **123** (2008) 012033.

[14] SNYDER, P.B., et al., “Progress in the peeling-ballooning model of edge localized modes: Numerical studies of nonlinear dynamics,” Phys. Plasmas **12** (2005) 056115.

[15] MAINGI, R., et al., “H-mode pedestal, ELM and power threshold studies in NSTX,” Nucl. Fusion **45** (2005) 1066.

[16] KASS, T., et al., “Characteristics of Type I and Type III ELM precursors in ASDEX Upgrade,” Nucl. Fusion **38** (1998) 111.

[17] LIANG, Y., et al., “Magnetic Topology Changes Induced by Lower Hybrid Waves and their Profound Effect on Edge-Localized Modes in the EAST Tokamak,” Phys. Rev. Lett. **110** (2013) 235002.